

# Interference in the scattering of Mössbauer radiation by $^{57}\text{Fe}$ nuclei located on nonequivalent positions, for Bragg reflection by a $\text{Fe}_3\text{BO}_6$ crystal

P. P. Kovalenko, V. G. Labushkin, A. K. Ovsepyan, É. R. Sarkisov, E. V. Smirnov, and I. G. Tolpekin

All-Union Scientific-Research Institute of Physicotechnical and Radio Engineering Measurements

(Submitted 28 November 1984)

Zh. Eksp. Teor. Fiz. **88** 1336–1347 (April 1985)

The diffraction of Mössbauer  $\gamma$  radiation by the weakly ferromagnetic crystal  $\text{Fe}_3\text{BO}_6$  has been investigated, and the interference of resonance nuclear scattering of Mössbauer  $\gamma$  quanta by iron nuclei located in the crystallographically nonequivalent  $4c$  and  $8d$  positions has been analyzed in detail. The energy spectra of pure nuclear Bragg reflection, from the (100) set of planes in a  $\text{Fe}_3\text{BO}_6$  crystal, of resonance  $\gamma$  radiation of the  $^{57}\text{Fe}$  isotope with an energy of 14.4 keV have been studied experimentally for odd orders of reflection. It is shown that the shape of the spectra obtained is determined by the nature of the interference of the scatterings by the  $^{57}\text{Fe}$  nuclei in the  $4c$  and  $8d$  positions, and the cases of constructive and destructive interference are investigated in detail. The results of the measurements are in good agreement with the theoretical spectra calculated for models of ideal and mosaic crystals. Possible applications of interference of resonance nuclear levels in structure investigations are discussed.

## INTRODUCTION

There has recently been appreciable interest in the study of the diffraction of resonance nuclear (Mössbauer)  $\gamma$  radiation by crystals (see, for example, Refs. 1–4 and the citations in them). This interest is connected, on the one hand, with possible application of the Mössbauer diffraction method in structural investigations, in particular for studying the crystal structure of materials, and also the structure of hyperfine fields at Mössbauer nuclei. On the other hand there is interest in studying new physical phenomena which arise at the diffraction of Mössbauer  $\gamma$  quanta in crystals, for example the effect of suppression of inelastic nuclear reaction channels,<sup>1,5–8</sup> or new features of phenomena already known, such as, for example, pendulum beats (Pendellosung) in Laue diffraction.<sup>9,10</sup> We note that the phenomena mentioned and, besides, a number of other features of the coherent scattering of Mössbauer radiation, show up most clearly under conditions of hyperfine splitting of a Mössbauer line in the crystal on, for example, scattering by magnetically ordered crystals.

Until recently, experimental studies of the diffraction of Mössbauer radiation by magnetically ordered crystals have been carried out mainly on crystals of  $\text{Fe}$ ,<sup>7</sup>  $\alpha\text{-Fe}_2\text{O}_3$ ,<sup>11,12</sup> and  $\text{FeBO}_3$ .<sup>13,14</sup> The use in experiment of a limited number of compounds possessing the same relatively simple crystallographic and magnetic structures, was characteristic of the initial stage of Mössbauer diffraction studies and was explained by the difficulty in obtaining single-crystal specimens, enriched in the Mössbauer isotope. Recently, in view of progress achieved in the technique of growing enriched single crystals,<sup>15</sup> magnetic crystals with a more complicated structure, containing several tens of atoms in the elementary cell, have started to be used in a Mössbauer diffraction experiment.<sup>16,17</sup> One such material, which is of interest for studying coherent scattering of Mössbauer radiation is iron borate  $\text{Fe}_3\text{BO}_6$ .

The crystal structure of  $\text{Fe}_3\text{BO}_6$  has been studied by White *et al.*<sup>18</sup> and by Diehl and Brandt;<sup>19</sup> analysis of the magnetic properties<sup>20–23</sup> showed that the crystal is a uniaxial antiferromagnet with weak ferromagnetism, with Néel point  $T_N = 508$  K.

An important feature of  $\text{Fe}_3\text{BO}_6$  is that the iron ions in this compound occur in two crystallographically nonequivalent types of site, the particular  $4c$  and general  $8d$ , for which the magnitude of the effective magnetic field at the iron nuclei, and also the structure of the electric field gradients (EFG) and the isomer shifts are different. This difference leads to the positions of the resonance lines for the iron nuclei in the  $4c$  and  $8d$  positions being, in general, different from one another. Near each resonant transition between the Zeeman sublevels of the ground and excited states of the nucleus  $m_i \rightarrow m_f$  (where  $m_i$  and  $m_f$  are the magnetic quantum numbers), the two resonance lines of the  $^{57}\text{Fe}$  nuclei corresponding to the  $4c$  and  $8d$  positions ( $c$  and  $d$  lines) thus give the main contribution to the  $\gamma$  quanta scattering. The energy difference between the  $c$  and  $d$  lines corresponding to one and the same Mössbauer transition is different for different transitions and, in addition, depends on specimen temperature.<sup>22,24</sup> The magnitude of the energy difference lies within the limits from  $\Gamma$  to  $\sim 10\Gamma$ , where  $\Gamma$  is the natural width of the Mössbauer line. On diffraction scattering, the contributions from the  $c$  and  $d$  lines interfere among themselves, which can lead to a noticeable change in the shape of the diffracted radiation line compared with the case of an isolated resonance.

The first experimental studies of the diffraction of Mössbauer  $\gamma$  radiation by a  $\text{Fe}_3\text{BO}_6$  single-crystal revealed the interference of  $c$  and  $d$  lines on scattering into nuclear magnetic diffraction maxima<sup>25</sup> and, in addition, made it possible to determine reliably the magnetic structure of the crystal.<sup>26</sup> It was shown, in particular, that on constructive interference a broadening, and on destructive interference a narrowing, of the combined resonance line is possible, com-

pared with the case of an isolated resonance.

In the present work a systematic study of the interference of  $c$  and  $d$  lines on Bragg reflection of Mössbauer radiation from a  $\text{Fe}_3\text{BO}_6$  crystal is carried out. A detailed analysis of the interference of two closely placed resonance lines in Mössbauer scattering is given. The influence of interference on the shape of the energy spectrum of the diffracted radiation, for the cases of constructive and destructive interference, is studied in detail. Results of the measurements are compared with theoretical calculations carried out for models of ideal and mosaic crystals. Possible applications of the interference of closely placed resonances lines in physical investigations are discussed.

#### EXPERIMENTAL METHOD. RESULTS OF THE MEASUREMENTS

The experimental investigations were carried out on a Mössbauer diffractometer, the design of which was de-

scribed before.<sup>26</sup> The  $\gamma$ -quanta beam with energy  $E = 14.4$  keV and line width  $\Gamma_s = 2\Gamma$  from a Mössbauer source  $^{57}\text{Co}(\text{Cr})$  of activity  $\sim 100$  mC, secured to the shaft of an electromagnetic vibrator, passed through a system of collimators and, with a divergence of  $\sim 0.8^\circ$ , fell on a  $^{57}\text{Fe}_3\text{BO}_6$  single crystal placed on a goniometer in one of the positions of symmetrical Bragg reflection  $(h, 0, 0)$ . In the experiment, reflections with odd values of  $h$  were studied (pure nuclear magnetic diffraction maxima), to which only resonance scattering by nuclei makes a contribution. The setting of the crystal in the reflecting Bragg position was carried out with the help of the bremsstrahlung from an x-ray tube, which could fall on the specimen studied through the hollow shaft of the vibrator.

In the method of adjusting the crystal for pure nuclear diffraction maxima,<sup>27</sup> for which structural extinction of Rayleigh scattering of 14.4 keV x rays occurs, use is made of the fact that the x radiation of energy 28.8 keV, such extinc-

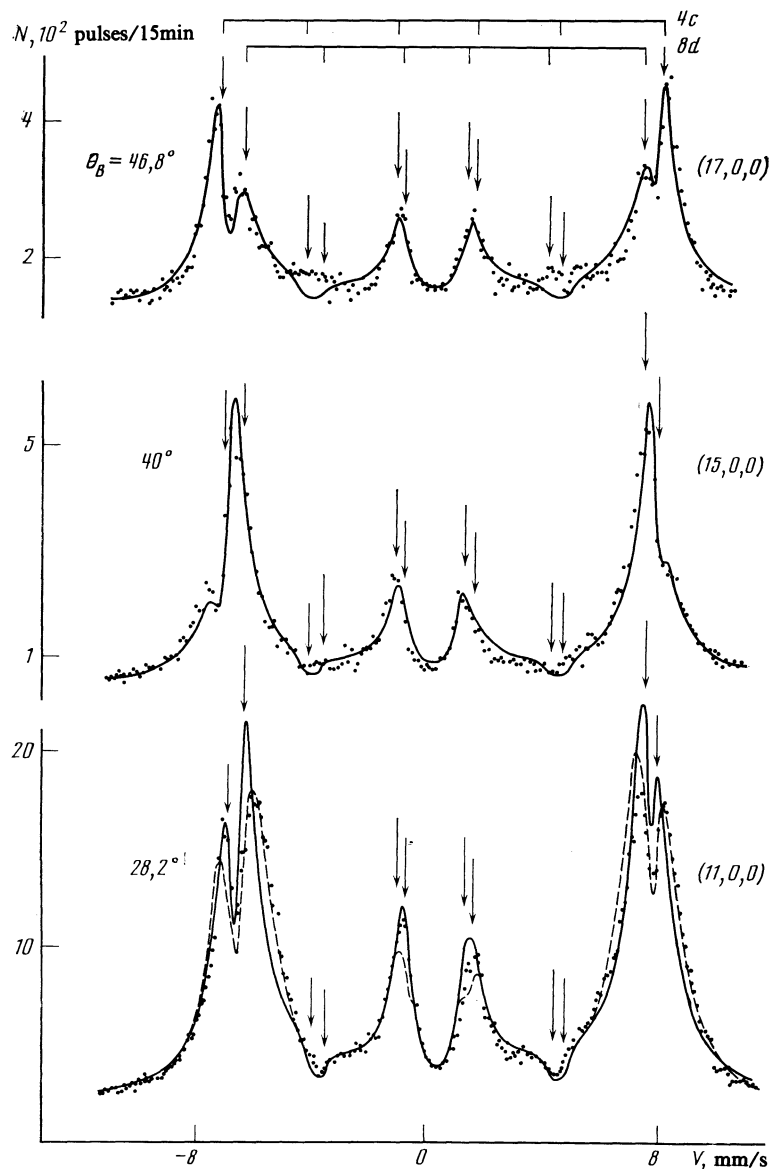


FIG. 1. Energy dependence of the intensity of  $\gamma$  radiation, diffracted by a  $^{57}\text{Fe}_3\text{BO}_6$  single-crystal, for the  $(11, 0, 0)$ ,  $(15, 0, 0)$  and  $(17, 0, 0)$  reflections corresponding to the case of constructive interference. The full and dashed lines show the theoretical spectra for the ideal and mosaic crystal models respectively. The vertical arrows give the positions of the resonances for iron nuclei in  $4c$  and  $8d$  positions,  $\theta_B$  is the Bragg angle

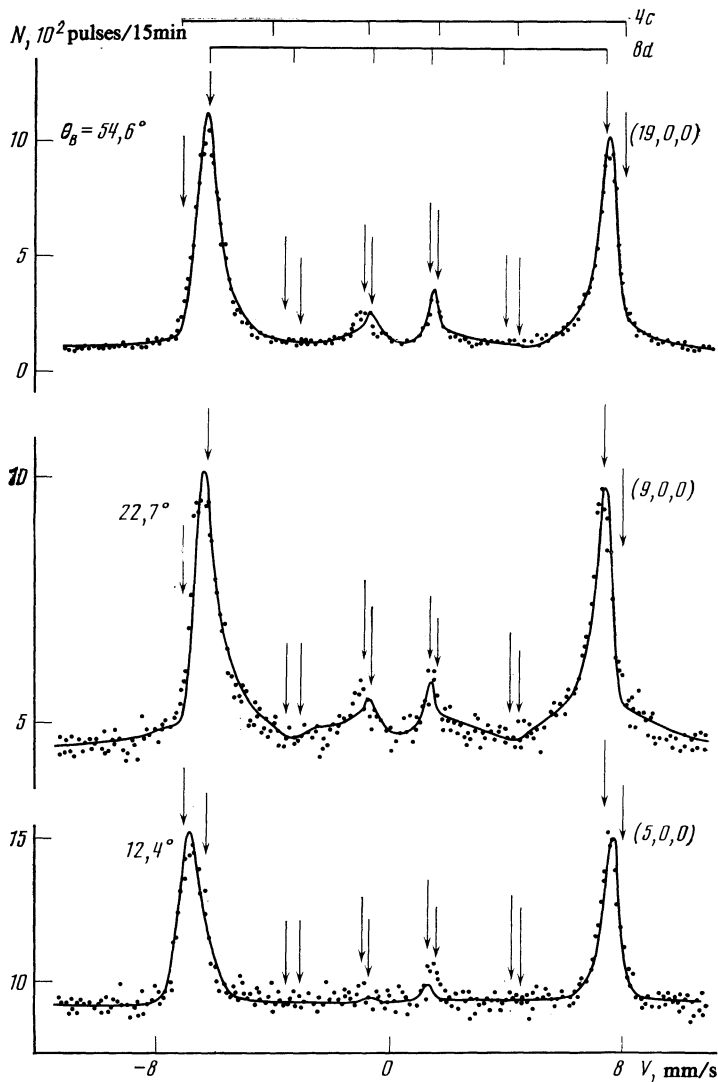


FIG. 2. Spectra for the (5, 0, 0), (9, 0, 0) and (19, 0, 0) reflections corresponding to the case of destructive interference.

tion does not take place. Adjustment is carried out by the second order of reflection with the help of a single-channel pulse-height analyzer. The diffracted radiation was recorded by an Si(Li) detector with energy resolution 250 eV for the  $\text{FeK}\alpha$  line and detector area of sensitive surface 100 mm<sup>2</sup>. All measurements were carried out at room temperature at constant velocities.

A  $\text{Fe}_3\text{BO}_6$  crystal with dimensions  $12 \times 6 \times 0.3$  mm, enriched in the resonance isotope  $^{57}\text{Fe}$  to 95%, was grown at the Simferopol State University.<sup>26</sup> The width of the rocking curve in the (4, 0, 0) reflection for  $\text{MoK}\alpha$  x radiation was  $20^\circ$ . A (100) plane emerged at the crystal surface, the weakly ferromagnetic moment lay along the [100] axis, the antiferromagnetic axis was in the (100) scattering plane and in the  $(\mathbf{k}_1, \mathbf{k}_2)$  plane, where  $\mathbf{k}_1$  and  $\mathbf{k}_2$  are the wave vectors of the incident and scattered waves.

The results of the experimental studies are shown in Figs. 1 and 2. Energy spectra of the (11, 0, 0), (15, 0, 0) and (17, 0, 0) reflections are shown in Fig. 1, corresponding to the case of constructive interference of the  $c$  and  $d$  lines, for

which the structure factors  $F_{\text{str}}^c$  and  $F_{\text{str}}^d$  for iron atoms respectively in the  $4c$  and  $8d$  positions have the same sign. The distinguishing feature of these spectra is the broadening of the resonance lines and also the existence of splitting of the outer lines in the spectrum.

The energy spectra of the (5, 0, 0), (9, 0, 0) and (19, 0, 0) reflections shown in Fig. 2 correspond to the case of destructive interference, for which  $F_{\text{str}}^c$  and  $F_{\text{str}}^d$  have different signs. In this case the resonance peaks have the shape of narrow single lines.

Theoretical calculations of Mössbauer diffraction by a  $\text{Fe}_3\text{BO}_6$  crystal were carried out for ideal and mosaic crystal models. Comparison of the theoretical curves with the experimental spectra was carried out by the least squares method, taking account of the contribution of all experimental points, unlike Artem'ev *et al.*,<sup>12</sup> who mainly took account of the nonresonance region of the spectrum in comparing the theoretical and experimental spectra of haematite. The spectra obtained reveal interesting features of the interference of two closely spaced resonance lines in the diffraction scatter-

ing of Mössbauer  $\gamma$ -quanta. Before going on to discuss them we present the results of a theoretical consideration of the diffraction of Mössbauer radiation by a  $\text{Fe}_3\text{BO}_6$  crystal.

### STRUCTURAL SCATTERING AMPLITUDE

The amplitude of the coherent scattering of Mössbauer  $\gamma$  radiation by an elementary cell of a crystal has the form

$$F_{rkl}^{(N)} = \sum_{j=1}^{12} F_j^{(N)} \exp\{i(\mathbf{k}_2 - \mathbf{k}_1) \mathbf{r}_j\}, \quad (1)$$

where  $F_j^{(N)}$  is the amplitude of the scattering by the  $j$ th Mössbauer nucleus,  $\mathbf{r}_j$  is its coordinate; the summation is carried out over all the resonance nuclei in the elementary cell. We note that the amplitude of Eq. (1) is written for scattering into the nuclear diffraction maximum and therefore does not contain a Rayleigh term.

Since the  $^{57}\text{Fe}$  nuclei in a  $\text{Fe}_3\text{BO}_6$  crystal are in the crystallographically nonequivalent  $4c$  and  $8d$  positions, it is convenient to divide the sum in Eq. (1) into two, in each of which the summation is over the nuclei in one position

$$F_{hkl}^{(N)} = \sum_{p=1}^4 F_p^{(N)c} \exp\{i(\mathbf{k}_2 - \mathbf{k}_1) \mathbf{r}_p^c\} + \sum_{q=1}^8 F_q^{(N)d} \exp\{i(\mathbf{k}_2 - \mathbf{k}_1) \mathbf{r}_q^d\}. \quad (2)$$

The indices  $c$  and  $d$  here denote quantities referring to Mössbauer nuclei corresponding to the  $4c$  and  $8d$  positions. In Eq. (2) it is also taken into account that four iron ions are in the  $4c$  positions while eight ions are in  $8d$  positions.

Carrying out the summation in Eq. (2) and taking into account all the hyperfine structure components, we obtain

$$F_{hkl}^{(N)} = f_0 \left[ F_{\text{str}}^c \sum_{n=1}^6 P_n^{(N)c} (E - E_n^c + i\Gamma/2)^{-1} + F_{\text{str}}^d \sum_{n=1}^6 P_n^{(N)d} (E - E_n^d + i\Gamma/2)^{-1} \right], \quad (3)$$

where

$$F_{\text{str}}^c = \sum_{p=1}^4 \exp\{i(\mathbf{k}_2 - \mathbf{k}_1) \mathbf{r}_p^c\}, \quad F_{\text{str}}^d = \sum_{q=1}^8 \exp\{i(\mathbf{k}_2 - \mathbf{k}_1) \mathbf{r}_q^d\},$$

$f_0$  is the common factor of the resonance nuclear amplitudes for iron nuclei in  $4c$  and  $8d$  positions,  $E$  is the  $\gamma$  radiation energy,  $P_n^{(N)}$  and  $E_n$  are, respectively, the nuclear polarization factor and resonance value of the energy for the  $n$ th resonance line in the spectrum, the index  $n$  enumerates the resonance lines of the  $^{57}\text{Fe}_3\text{BO}_6$  spectrum in the direction of increasing  $E$ .

Since the magnetic fields at the iron nuclei in each of the positions are ordered antiferromagnetically,<sup>1),20,26</sup> then  $P_n^{(N)c} = P_n^{(N)d} = P_n^{(N)}$ , where

$$P_n^{(N)} = (\mathbf{n}_1 \mathbf{h}_n^*(\mathbf{k}_1)) (\mathbf{h}_n(\mathbf{k}_2) \mathbf{n}_2^*) - (\mathbf{n}_1 \mathbf{h}_n(\mathbf{k}_1)) (\mathbf{h}_n^*(\mathbf{k}_2) \mathbf{n}_2^*). \quad (4)$$

In Eq. (4)  $\mathbf{n}_1$  and  $\mathbf{n}_2$  are the polarization vectors corresponding to the incident and scattered radiation,  $\mathbf{h}_n(\mathbf{k}_i)$  is the po-

larization vector of the radiation emitted in direction  $\mathbf{k}_i$  in the Mössbauer transition indicated by the index  $n$ . The explicit form of  $\mathbf{h}_n(\mathbf{k}_i)$  and the factor  $f_0$  can be found, for example, in Belyakov.<sup>2</sup>

Equation (3), with Eq. (4) taken into account, gives the amplitude  $F_{hkl}^{(N)}(\mathbf{n}_1, \mathbf{n}_2)$  of coherent scattering of a wave with polarization  $\mathbf{n}_1$  into a wave with polarization  $\mathbf{n}_2$ . The expressions which determine the intensity of diffraction scattering  $I_R(\mathbf{n}_1, \mathbf{n}_2)$  through the amplitude  $F_{hkl}^{(N)}(\mathbf{n}_1, \mathbf{n}_2)$  for the cases of ideal and mosaic crystals are well known.<sup>2,28</sup> We shall make use of these expressions without quoting them here.

If the incident beam of  $\gamma$  quanta is unpolarized, then  $I_R(\mathbf{n}_1, \mathbf{n}_2)$  must be averaged over the polarizations. For the experimental conditions chosen (scattering into the nuclear magnetic maxima, antiferromagnetic axis lying in the  $(\mathbf{k}_1, \mathbf{k}_2)$  plane), averaging over polarizations amounts to summation of the intensities of the diffraction scattering corresponding to  $\pi$ - and  $\sigma$ -polarized  $\gamma$  quanta falling on the crystal, since in the present case these two polarizations are scattered independently of one another. We should remember that the  $\pi$ -polarization lies in the  $(\mathbf{k}_1, \mathbf{k}_2)$  plane, while the  $\sigma$  polarization is perpendicular to this plane.

It is interesting to note that the polarization properties of  $P_n^{(N)}$  are in this case such that the diffraction scattering of  $\gamma$  quanta takes place only with rotation of the plane of polarization. For example, if  $\pi$ -polarized radiation falls on the crystal, then the diffracted beam will consist only of  $\sigma$ -polarized  $\gamma$  quanta, and on the other hand a  $\sigma$ -polarized incident beam gives only  $\pi$ -polarized  $\gamma$  quanta on scattering. This results from the amplitudes of nuclear scattering without change of polarization,  $F_{hkl}^{(N)}(\pi_1, \pi_2)$  and  $F_{hkl}^{(N)}(\sigma_1, \sigma_2)$  being zero in the case considered, while the scattering amplitudes for a change in polarization,  $F_{hkl}^{(N)}(\pi_1, \sigma_2)$  and  $F_{hkl}^{(N)}(\sigma_1, \pi_2)$ , differ from zero. Analysis of Eqs. (3) and (4) shows that for the experimental geometry chosen  $F_{hkl}^{(N)}(\pi_1, \sigma_2) = -F_{hkl}^{(N)}(\sigma_1, \pi_2)$ .

### MODEL OF TWO LINES

As has already been noted above, two resonance lines make the main contribution to the scattering near each Mössbauer transition, one for iron nuclei in  $4c$  positions, the other for nuclei in the  $8d$  positions. In the present section, therefore, we introduce the results of a numerical calculation for two resonance lines for an analysis of Mössbauer scattering by crystals in which the resonance nuclei are in nonequivalent positions.

We write the scattering amplitude in the form

$$F^{(N)} = F_1^{(N)} + F_2^{(N)} = a_1 [2(E - E_1)/\Gamma + i]^{-1} + a_2 [2(E - E_2)/\Gamma + i]^{-1}, \quad (5)$$

where  $a_1$  and  $a_2$  give the contribution to the scattering from each resonance line (i.e., they play the role of the structure factors in Eq. (3)), and  $E_1$  and  $E_2$  determine the positions of these lines. In what follows we will use the parameter  $\Delta = E_2 - E_1$ , determining the distance between the lines.

For definiteness we will calculate the diffracted beam intensity  $I_R$  on the model of a mosaic crystal<sup>28</sup> with subsequent averaging over the shape of the source line. The results

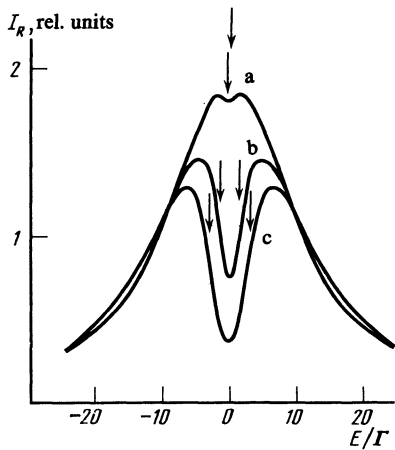


FIG. 3. Diffraction spectra for constructive interference for three values of the parameter  $\Delta$ : a)  $\Delta = 0.5\Gamma$ , b)  $\Delta = 3\Gamma$ , c)  $\Delta = 6\Gamma$ . The case of equal amplitudes  $a_1 = a_2 = 1$ .

of the calculations are shown in Figs. 3–6.

The dependence of  $I_R$  on  $\gamma$ -radiation energy is shown in Fig. 3 for the case of constructive interference with an equal contribution from each line. The calculated curves are obtained for three values of the parameter  $\Delta$ ; the vertical arrows give the positions of the resonances for each value of  $\Delta$ , the widths of the source lines is assumed to be equal to  $2\Gamma$ . The value of the coefficient of linear attenuation of the  $\gamma$  quanta by electrons  $\mu_e$  and nuclei  $\mu_N$  was taken to be the same as for a  $\text{Fe}_3\text{BO}_6$  crystal.

For constructive interference the existence of resonance coefficients for the amplitudes  $F_1^{(N)}$  and  $F_2^{(N)}$  in Eq. (5) leads to the real parts of  $F_1^{(N)}$  and  $F_2^{(N)}$  adding together in the region of  $\gamma$ -ray energies to the right and left of both resonances, and subtracting in the energy region lying between the resonances. This means that the diffraction scattering of  $\gamma$  quanta is increased to the left and right of the resonances, while it is weakened between the resonances. For values of  $\Delta < \Gamma/2$  the

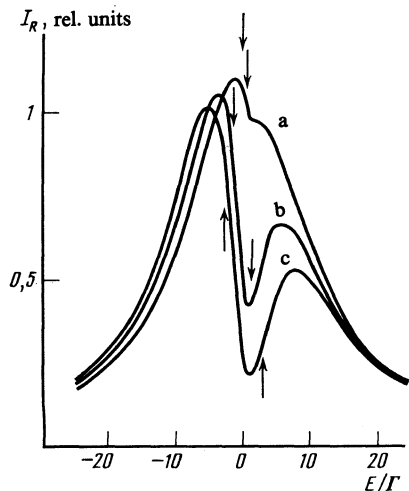


FIG. 4. Spectra for constructive interference in the case of unequal amplitudes:  $a_1 = 1$ ,  $a_2 = 0.5$ . The values of  $\Delta$  are the same as in Fig. 3.

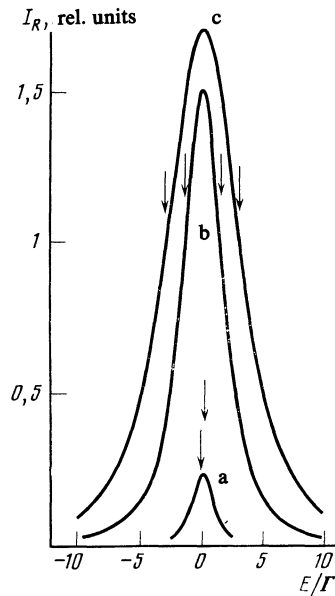


FIG. 5. The shape of the diffraction spectra for destructive interference in the case of equal amplitudes:  $a_1 = 1$ ,  $a_2 = -1$ . The values of  $\Delta$  are the same as in Fig. 3.

dimensions of the region where  $F_1^{(N)}$  and  $F_2^{(N)}$  cancel one another is small and the function  $I_R(E)$  has the form of a single line with smoothed-out vertex. For  $\Delta \geq \Gamma/2$  a dip appears in the center of the diffracted spectrum (Fig. 3, a), which grows as  $\Delta$  increases. In this case  $I_R$  as a function of  $E$  has a “volcano-like” shape, in which the inner slope is steeper than the outer. For values of  $\Delta = 3\Gamma$  and  $6\Gamma$  the diffraction spectra have two peaks, the distance between which is more than double the distance between the resonance lines (Figs. 3, b, c). For given values of  $\Delta$ , constructive interference thus leads to an anomalous splitting of the spectrum of diffracted radiation.

The difference between the amplitudes  $a_1$  and  $a_2$  in Eq. (5) leads to an asymmetry of the spectrum. The curves shown

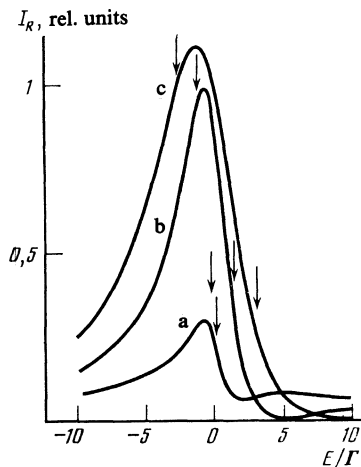


FIG. 6. Diffraction spectra for destructive interference in the case of unequal amplitudes:  $a_1 = 1$ ,  $a_2 = -0.5$ . The values of  $\Delta$  are the same as in Fig. 3.

in Fig. 4 demonstrate this clearly. It should be remarked that the peak in the spectrum of diffracted radiation, corresponding to the line of smaller amplitude is shifted further from its resonance position than for the line with larger amplitude.

For destructive interference, when the amplitudes  $a_1$  and  $a_2$  have different signs, the diffraction scattering increases in the energy region between the resonances and is weaker outside it. The corresponding spectra of the diffracted radiation are shown in Fig. 5 for the case of equal contributions from each line. The  $I_R(E)$  dependence of Fig. 5 has the shape of a single symmetrical peak, differing from a Lorentzian by a sharper vertex and a more rapid fall in the wings. The maximum value of  $I_R(E)$  is reached exactly between the resonances. Destructive interference leads to a noticeable compression of the diffracted spectrum, the width of which, as shown by calculation, can be less than the width of the diffracted spectrum of a single Mössbauer line.

The shape of the spectrum in the case of unequal contributions of destructively interfering resonance lines is shown in Fig. 6. The curves shown reveal the asymmetry of the diffraction spectrum and display a steeper fall in  $I_R(E)$  on the side of the smaller amplitude resonance. We note that in this case the maximum of  $I_R(E)$  is reached for values of  $E$  closer to  $E_1$ , i.e., to the position of the resonance line of larger amplitude.

The model of two lines discussed in the present section clearly demonstrates the influence of interference on the shape of the energy spectrum of diffracted  $\gamma$  radiation. It should be noted that this model can be used not only for purposes of illustration, but also in calculating spectra for concrete experimental situations. In particular, it is applicable in those cases where the distance between the interfering lines,  $\Delta$ , is small while the energy of the  $\gamma$  quanta lies near the resonance values  $E_1$  and  $E_2$ . The contribution of the remaining lines of the spectrum can then only give an insignificant (a few percent<sup>29</sup>) correction to the scattering intensity. The approximation of two lines thus not only simplifies the discussion, but also can give a good quantitative description of the resonance region of the spectrum.

## DISCUSSION OF THE RESULTS

As the results of the previous section have shown, the shape of the diffraction spectrum is determined to an appreciable extent by the relation between the structure factors for iron nuclei in the  $4c$  and  $8d$  positions. The values of  $F_{str}^c$  and  $F_{str}^d$  for  $^{57}\text{Fe}$  nuclei in the  $4c$  and  $8d$  positions for  $(h, 0, 0)$  reflections from a  $\text{Fe}_3\text{BO}_6$  crystal are given below:

$(h, 0, 0)$	(5, 0, 0)	(9, 0, 0)	(11, 0, 0)	(15, 0, 0)	(17, 0, 0)	(19, 0, 0)
$I_{str}^c$	3,70	-0,94	-3,90	1,54	3,98	2,08
$I_{str}^d$	-5,04	4,48	-6,80	7,14	3,32	-7,42

It should be noted that the structure factors for  $(h, 0, 0)$  reflections, where  $h$  is an odd number, are real numbers and for different values of  $h$  can differ not only in magnitude but also in sign. For each of the reflections (11, 0, 0), (15, 0, 0) and (17, 0, 0) the signs of  $F_{str}^c$  and  $F_{str}^d$  agree among themselves, which leads to constructive interference of the  $c$  and  $d$  lines. For the reflections (5, 0, 0), (9, 0, 0) and (19, 0, 0) the signs of

$F_{str}^c$  and  $F_{str}^d$  are opposite, which leads to destructive interference.

Yet another parameter which has a noticeable influence on the form of the spectrum is the energy difference between the  $c$  and  $d$  lines of the separate components of the hyperfine structure  $\Delta_n = E_n^d - E_n^c$ . The values of  $\Delta_n$  for the Mössbauer transitions in  $^{57}\text{Fe}$  nuclei in  $4c$  and  $8d$  positions, expressed in units of  $\Gamma$ , are given below:

$n$	1	2	3	4	5	6
$\Delta_n$	5,9	2,8	0,5	-1,3	-3,6	-3,3

It is convenient to analyze the spectra with the help of the results obtained in the previous section.<sup>2)</sup> We shall at first discuss constructive interference of the  $c$  and  $d$  lines. The effect of interference on the shape of the diffraction spectrum is a maximum for the (11, 0, 0) and (17, 0, 0) reflections for which  $F_{str}^c$  and  $F_{str}^d$  are large and comparable in magnitude. For these reflections there is an anomalous splitting of the outer lines in the spectrum and a broadening of them to  $\sim 20\Gamma$ . The third and fourth lines in the spectrum are also broadened but not split, since the values of  $\Delta_3$  and  $\Delta_4$  corresponding to them are small. Because  $|\Delta_3| < |\Delta_4|$ , the intensity of the diffraction scattering for the third line is greater than for the fourth.  $F_{str}^d$  for the (15, 0, 0) reflection is appreciably greater than  $F_{str}^c$ , so that the influence of interference is clearly marked in this case.

It should be noted that for nearly all  $(h, 0, 0)$  reflections from a  $\text{Fe}_3\text{BO}_6$  crystal ( $h$  an odd integer) the absolute value of the structure factors for iron nuclei in  $8d$  positions are greater than for nuclei in  $4c$  positions. This is not surprising since there are twice as many iron nuclei in  $8d$  positions as in  $4c$  positions. The only exception is the (17, 0, 0) reflection for which  $|F_{str}^c| > |F_{str}^d|$ . In the split outer peaks of the spectra of the (11, 0, 0) and (15, 0, 0) reflections, therefore, the lines corresponding to scattering by iron nuclei in  $8d$  positions are more intense, while in the (17, 0, 0) spectrum it is the lines corresponding to scattering by nuclei in  $4c$  positions.

Since scattering of Mössbauer  $\gamma$  radiation in nuclear magnetic diffraction maxima are studied in this work, there are no contributions to the scattering from transitions with  $\Delta m = 0$ , where  $\Delta m = m_f - m_i$ . Near these transitions (the second and fifth lines in the spectrum) the intensity of the reflected radiation has small dips produced by absorption of the  $\gamma$  radiation in these transitions on scattering at zero angle.<sup>29</sup>

The theoretical curves shown in Fig. 1 show good agreement with the experimental results. The theoretical spectra for the (15, 0, 0) and (17, 0, 0) reflections, calculated on the ideal and mosaic crystal models agree, but there is a small difference between them for the (11, 0, 0) reflection. We note that for the (17, 0, 0) reflection near transitions with  $\Delta m = 0$  there is some difference between the theoretical and experimental spectra. The theoretical spectrum near transitions with  $\Delta m = 0$  has small dips, while there are no dips in the experimental spectrum. The reason for this discrepancy remains to be explained.

For destructive interference all the lines in the spectrum of diffracted radiation are in the form of single narrow peaks (Fig. 2). The peaks in the spectrum in the case of the (5, 0, 0)

reflection, for which  $|F_{str}^d|$  and  $|F_{str}^c|$  are close in magnitude, have an almost symmetrical shape, with the maximum of each of them lying between the corresponding  $c$  and  $d$  lines. For the (9, 0, 0) and (19, 0, 0) lines,  $|F_{str}^d| > |F_{str}^c|$ , so that the peaks in the energy dependences have an asymmetric shape, and their maxima are close to the corresponding values of  $E_n^d$ .

A characteristic feature of diffraction spectra in the case of destructive interference is that the peak for the first line in the spectrum is broader than for the sixth. This is related to the fulfillment of the inequality  $|\Delta_1| > |\Delta_6|$ , i.e., to the fact that the region over which scattering through the  $c$  and  $d$  lines enhances each other is greater for the first line than for the sixth. A similar inequality for the inner lines of the spectrum,  $|\Delta_4| > |\Delta_3|$  leads to the peak for the fourth line being more intense than for the third.

The width of the peaks of the spectra shown in Fig. 2 is appreciably less than for the case of constructive interference. In addition, the separate peaks are narrower than in the case of scattering through a single line (isolated resonance). For example, calculations show that for the (5, 0, 0) reflection the peak for the sixth line in the spectrum is about twice as narrow as for the same line on scattering only by iron nuclei in  $8d$  positions.

It should be noted that the dips near transitions with  $\Delta m = 0$  are almost absent for destructive interference. This is a result of weakening of diffraction scattering due to interference of the  $c$  and  $d$  lines in the wings of the spectrum.

Theoretical spectra calculated on the ideal and mosaic crystal models agree in the case of destructive interference for all reflections studied and agree well with the results of the experimental observations.

## CONCLUSIONS

The results of the present work show that a  $Fe_3BO_6$  crystal offer convenient and promising material for studying the interference of closely spaced nuclear resonant transitions. It is possible with this crystal to study both constructive and destructive interference for different contributions of interfering lines. The shape of the diffraction spectra for each reflection together with general relationships have a number of characteristic features containing information about the scattering crystal. For example, the dependence of the diffraction picture on the contributions of the  $c$  and  $d$  lines can be used to determine the structure factors  $F_{str}$ , i.e., for studying the crystal structure of the material. This same dependence can also, in principle, be used to study impurity compounds to determine the position of the impurity atoms and their inclusion in the matrix. The high sensitivity of the interference picture to the type of magnetic ordering in the crystal should also be noted, making it possible to demonstrate a clear and simple means of determining the magnetic structure of  $Fe_3BO_6$  with the help of magnetic Mössbauerography.<sup>26</sup>

The results of the present work show a number of interesting features of the Mössbauer diffraction method of structural studies in the presence of interference of the resonant nuclear lines. We should especially stress the merits of this

method in studying compounds with complicated crystal-line and magnetic structures in those cases when application of traditional methods of structural analysis—x-ray and neutron diffraction—is inconvenient. The results obtained can be used in studying diffraction scattering of Mössbauer radiation from other compounds, particularly those in which the Mössbauer nuclei are in non-equivalent positions.

The authors thank V. N. Seleznev and A. R. Prokopov who grew the isotopically enriched crystals, and E. A. Aris-tov and V. A. Bakhshi-Zade for help in carrying out the computer calculations.

<sup>1</sup>For the further discussion, the weak ferromagnetism of the  $Fe_3BO_6$  crystal is insignificant.

<sup>2</sup>It should be borne in mind, however, that the theoretical spectra shown in Figs. 1 and 2 were calculated by taking into account the contribution of all the hyperfine structure components.

<sup>1</sup>Yu. Kagan and A. M. Afanas'ev in: Mössbauer Spectroscopy and its Applications, IAEA, Vienna (1972) p. 143.

<sup>2</sup>V. A. Belyakov, Usp. Fiz. Nauk **115**, 553 (1975) [Sov. Phys. Usp. **18**, 267 (1975)].

<sup>3</sup>V. G. Baryshevskii, Nuclear Optics of Polarized Media, BGU Press, Minsk (1976).

<sup>4</sup>M. A. Andreeva and R. N. Kuz'min, Mössbauer Gamma-Optics, MGU Press, Moscow (1982).

<sup>5</sup>A. M. Afanas'ev and Yu. Kagan, Zh. Eksp. Teor. Fiz. **48**, 327 (1965) [Sov. Phys. JETP **21**, 215 (1965)].

<sup>6</sup>A. M. Afanas'ev and Yu. Kagan, Zh. Eksp. Teor. Fiz. **64**, 1958 (1973) [Sov. Phys. JETP **37**, 987 (1973)].

<sup>7</sup>G. V. Smirnov, N. A. Semioshkina, V. V. Sklyarevskii, S. Kadechkova, and B. Shestak, Zh. Eksp. Teor. Fiz. **71**, 2214 (1976) [Sov. Phys. JETP **44**, 1167 (1976)].

<sup>8</sup>U. Van Bürck, G. V. Smirnov, R. L. Mössbauer, H. J. Maurus, and N. A. Semioshkina, J. Phys. C **13**, 4511 (1980).

<sup>9</sup>G. V. Smirnov, V. V. Sklyarevskii, and A. N. Artem'ev, Pis'ma Zh. Eksp. Teor. Fiz. **11**, 579 (1970) [JETP Lett. **11**, 400 (1970)].

<sup>10</sup>V. A. Belyakov, V. G. Labushkin, V. A. Sarkisyan, and E. V. Smirnov, Acta Crystallogr. Sect. A **34**, S227 (1978).

<sup>11</sup>G. V. Smirnov, V. V. Sklyarevskii, R. A. Voskanyan, and A. N. Artem'ev, Pis'ma Zh. Eksp. Teor. Fiz. **9**, 123 (1969) [JETP Lett. **9**, 70 (1969)].

<sup>12</sup>A. N. Artem'ev, I. P. Perstnev, V. V. Sklyarevskii, G. V. Smirnov, and E. P. Stepanov, Zh. Eksp. Teor. Fiz. **64**, 261 (1973) [Sov. Phys. JETP **37**, 136 (1973)].

<sup>13</sup>P. P. Kovalenko, V. G. Labushkin, V. V. Rudenko, V. A. Sarkisyan, and V. N. Seleznev, Pis'ma Zh. Eksp. Teor. Fiz. **26**, 92 (1977) [JETP Lett. **26**, 85 (1977)].

<sup>14</sup>G. V. Smirnov, V. V. Mostovoï, Yu. V. Shvyd'ko, V. N. Seleznev, and V. V. Rudenko, Zh. Eksp. Teor. Fiz. **78**, 1196 (1980) [Sov. Phys. JETP **51**, 603 (1980)].

<sup>15</sup>V. G. Labushkin and V. N. Seleznev, Proceedings of 2nd All-Union Conference on Methods and Apparatus for Studying Coherent Interaction of Radiation in Matter, Erevan (1982) p. 90.

<sup>16</sup>N. Hayashi and I. Sakamoto, Jpn. J. Appl. Phys. **16**, 1713 (1977).

<sup>17</sup>P. P. Kovalenko, V. G. Labushkin, A. R. Prokopov, É. R. Sarkisov, and V. N. Seleznev, Proc. 2nd All-Union Conf. on Methods and Apparatus for Studying Coherent Interaction of Radiation in Matter, Erevan (1982) p. 79.

<sup>18</sup>J. G. White, A. Miller, and R. E. Nielsen, Acta Crystallogr. **19**, 1060 (1965).

<sup>19</sup>R. Diehl and G. Brandt, Acta Crystallogr. Sect. B **31**, 1662 (1975).

<sup>20</sup>V. I. Mal'tsev, E. P. Naïden, S. M. Zhilyakov, R. P. Smolin, and L. M. Borisyyuk, Kristallografiya **21**, 113 (1976) [Sov. Phys. Crystallogr. **21**, 58 (1976)].

<sup>21</sup>O. A. Bayukov, V. M. Buznik, V. P. Ikonnikov, M. I. Petrov, and M. A. Popov, Fiz. Tverd. Tela (Leningrad) **18**, 2435 (1976) [Sov. Phys. Solid State **18**, 1421 (1976)].

<sup>22</sup>R. Wolfe, R. D. Pierce, M. Eibschütz, and J. W. Nielsen, Solid State Commun. **7**, 949 (1969).

<sup>23</sup>C. Voigt and D. Bonnenberg, Physica (Utrecht) **80**, 439 (1975).

<sup>24</sup>O. A. Bayukov, V. P. Ikonnikov, M. I. Petrov, V. N. Seleznev, R. P. Smolin, and V. V. Uskov, Pis'ma Zh. Eksp. Teor. Fiz. **14**, 49 (1971)

[JETP Lett. **14**, 32 (1971)].

<sup>25</sup>P. P. Kovalenko, V. G. Labushkin, A. K. Ovsepyan, É. R. Sarkisov, and E. V. Smirnov, Pis'ma Zh. Eksp. Teor. Fiz. **39**, 471 (1984) [JETP Lett. **39**, 573 (1984)].

<sup>26</sup>P. P. Kovalenko, V. G. Labushkin, A. K. Ovsepyan, É. R. Sarkisov, E. V. Smirnov, A. R. Prokopov, and V. N. Seleznev, Fiz. Tverd. Tela (Leningrad) **26**, 3068 (1984) [Sov. Phys. Solid State **26**, 1849 (1984)].

<sup>27</sup>V. G. Labushkin and V. A. Sarkisyan, Patent No. 714254, BI No. 5,

appl. July 15, 1977, publ. Feb. 5, 1980.

<sup>28</sup>Yu Kagan, A. M. Afanas'ev, and I. P. Perstnev, Zh. Eksp. Teor. Fiz. **54**, 1530 (1968) [Sov. Phys. JETP **27**, 819 (1968)].

<sup>29</sup>E. P. Stepanov, A. N. Artem'ev, I. P. Perstnev, V. V. Sklyarevskii, and G. V. Smirnov, Zh. Eksp. Teor. Fiz. **66**, 1150 (1974) [Sov. Phys. JETP **39**, 562 (1974)].

Translated by R. Berman